Hindawi Publishing Corporation
Advances in Mechanical Engineering
Volume 2012, Article ID 167296, 11 pages
doi:10.1155/2012/167296

Research Article

Natural Convection of Nanofluids in a Square Enclosure with a Protruding Heater

J. Guiet,[1] M. Reggio,[1,2] and P. Vasseur[1,3]

[1] *Ecole Polytechnique, Université de Montréal, C.P. 6079, Succ. "Centre Ville", Montréal, QC, Canada H3C 3A7*
[2] *Département de Génie Mécanique, École Polytechnique, Université de Montréal, C.P. 6079, Succ. "Centre Ville", Montréal, QC, Canada H3C 3A7*
[3] *Laboratoire des Technologies Innovantes, Université de Picardie Jules Verne d'Amiens, rue des facultés, le Bailly, 80025 Amiens Cedex, France*

Correspondence should be addressed to M. Reggio, marcelo.reggio@polymtl.ca

Received 17 March 2011; Accepted 26 June 2011

Academic Editor: Yogesh Jaluria

This paper reports a numerical study on natural convection from a protruding heater located at the bottom of a square cavity filled with a copper-water nanofluid. The vertical walls of the cavity are cooled isothermally; the horizontal ones are adiabatic, and the heater is attached to the bottom wall. The heat source is assumed either to be isothermal or to have a constant heat flux. The effective viscosity and thermal conductivity of the nanofluid are modeled according to Brinkman and Patel, respectively. Numerical solutions of the full-governing equations, based on the lattice Boltzmann method, are obtained for a wide range of the governing parameters: the Rayleigh number, Ra; the Prandtl number, Pr; the geometrical parameters specifying the heater; the volume fraction of nanoparticles, Φ. For a particular geometry, it has been found that, for a given Ra, heat transfer is enhanced with increasing Φ, independently of the thermal boundary condition applied on the heater.

1. Introduction

The convection of nanofluids, which are a mixture of nanoparticles in a base fluid [1], has recently been an active field of research, because of reports of greatly enhanced thermal properties. Compared with other techniques for enhancing heat transfer in practical applications, nanofluids have the advantage of behaving like pure fluids, because of the small size of nanoparticles. As a result, the possibility of using them as heat transfer fluids for various applications, such as advanced nuclear systems or microchannel and minichannel heat sinks, is currently under consideration.

A review of the literature (see, e.g., Godson et al. [2]) indicates that most studies on this topic are concerned mainly with forced convection applications, but relatively little attention has been devoted to the natural convection of nanofluids. The first study on the natural convection of a nanofluid confined in a differentially heated enclosure seems to be that of Khanafer et al. [3]. The same problem was considered by Jou and Tzeng [4]. The Khanafer et al. model was used to investigate convective heat transfer enhancement in rectangular enclosures filled with an Al_2O_3-water nanofluid. It was reported that increasing the buoyancy parameter and volume fraction causes an increase in the average heat transfer coefficient. Heat transfer in nanofluids by natural convection in a square cavity heated isothermally from the vertical sides has been investigated numerically by Ho et al. [5] and Santra et al. [6]. Two different formulas have been considered by Ho et al. [5], for the effective viscosity, and thermal conductivity of the nanofluids, while the Ostwald-de Waele model for a non-Newtonian shear-thinning fluid has been used by Santra et al. [6] to calculate the shear stress. It was found that the uncertainties associated with the various expressions adopted to model nanofluids have a major influence on the characteristics of heat transfer by natural convection in the enclosure. Heat transfer enhancement in a differentially heated enclosure using the variable thermal conductivity and variable viscosity of Al_2O_3-water and Cu-water nanofluids has been investigated numerically by Abu-Nada et al. [7]. The impact of both variable viscosity and

variable thermal conductivity, derived from experimental data, has been studied. It was observed that, at high Rayleigh numbers, the Nusselt number is more sensitive to viscosity models than to thermal conductivity models. Numerical study of natural convection in partially heated rectangular enclosures has been performed by Abu-Nada et al. [8]. Different types of nanoparticles were tested. They found that the heater location affects the flow and temperature fields when nanofluids are used. The same configuration was considered recently by Ghasemi and Aminossadati [9] for the case of an oscillating heat source embedded on the vertical wall of the enclosure. Recently, Alloui et al. [10] investigated natural convection, both analytically and numerically, in a shallow rectangular cavity filled with nanofluids. The critical Rayleigh number for the onset of supercritical convection of nanofluids is predicted explicitly by these authors. Also, results are obtained from the analytical model for finite amplitude convection for which the flow and heat transfer are presented in terms of the governing parameters of the problem.

Natural convection heat transfer in partially divided cavities filled with ordinary fluids has been the subject of many studies in the past, because of its importance in many engineering fields. Applications include thermal control of electric components, nuclear reactors, and so forth. Moukalled and Acharya [11] and Moukalled and Darwish [12] numerically investigated buoyancy-induced heat transfer in partially divided trapezoidal cavities representing attic spaces. The effects of the Rayleigh number, baffle height, and baffle location on heat transfer were discussed for various thermal boundary conditions. An experimental investigation concerning laminar convection in a box, with differentially heated end walls, which is divided by a barrier into two connected chambers, was carried out by Coman et al. [13]. They found that heat transfer diminishes rapidly when the barrier is high and also that it changes little when the lateral position of the barrier varies. Oztop and Bilgen [14] studied heat transfer numerically in a differentially heated and partitioned square cavity containing heat-generating fluid. It was found that the flow field and heat transfer are modified considerably with partial dividers. Natural convection heat transfer from a protruding heater located in a triangular enclosure has been analyzed numerically by Varol et al. [15]. They reported that, in order to obtain better heat removal, the heater must be located at the center of the bottom wall. The same problem was considered by AlAmiri et al. [16] for the case of a square cavity. Their investigation revealed that, as well as location, increasing the height and width of the heater results in the enhancement of heat transfer owing to the increase in the surface area of the heater. All the above investigations are concerned only with partially divided enclosures filled with ordinary fluids. To the author's knowledge, the influence of nanofluids on this flow configuration has not yet been studied.

In our investigation here, we consider natural convection in a square enclosure with a protruding heater subjected to various thermal boundary conditions. A numerical study is carried out to predict the effect of the location and dimension of the heat source on the flow and temperature fields in a cavity filled with a Cu-water nanofluid. The paper is organized as follows. The formulation of the problem and the numerical method are presented in Sections 2 and 3, respectively. In Section 4, the results obtained for the flow and heat transfer are discussed in terms of the geometry of the system. The final last section presents some concluding remarks related to optimum heat transfer enhancement based on the nanoparticle volume fraction, the length and the width of the enclosure, the Rayleigh number, and the location of the protruding heater.

2. Mathematical Formulation

Figure 1(a) schematically represents the flow configuration with a coordinate system. The square enclosure is of height H'. The vertical walls of the enclosure are cooled isothermally, at temperature T_c', while the horizontal walls are adiabatic. A protruding heater of height l' and width w' is placed at a distance d' from the left wall, as shown in the graph. The cavity is filled with Newtonian, incompressible nanofluid. The thermophysical properties of the mixture considered in this study are assumed constant, except for the density variation, which is determined based on the Boussinesq approximation. Also, it is supposed that the base fluid and the nanoparticles are in thermal equilibrium and that no slip occurs between them.

The governing macroscopic equations that describe the system behavior are those of conservation of mass, momentum, and energy, which are given as

$$\begin{aligned}
&\frac{\partial^2\Psi'}{\partial x'^2}+\frac{\partial^2\Psi'}{\partial y'^2}=-\omega',\\
&\frac{\partial\omega'}{\partial t'}+u'\frac{\partial\omega'}{\partial x'}+v'\frac{\partial\omega'}{\partial y'}\\
&\qquad=\frac{1}{\rho_{\mathrm{nf}}}\left[\mu_{\mathrm{nf}}\left(\frac{\partial^2\omega'}{\partial x'^2}+\frac{\partial^2\omega'}{\partial y'^2}\right)+\left(\rho\beta'\right)_{\mathrm{nf}}g\frac{\partial T'}{\partial x'}\right],\\
&\frac{\partial T'}{\partial t'}+u'\frac{\partial T'}{\partial x'}+v'\frac{\partial T'}{\partial y'}=\alpha_{\mathrm{nf}}\left(\frac{\partial^2 T'}{\partial x'^2}+\frac{\partial^2 T'}{\partial y'^2}\right),
\end{aligned}\tag{1}$$

in terms of stream function Ψ', vorticity ω', and temperature T'. As usual, in order to satisfy the continuity equation, the stream function Ψ' is defined such that $u'=\partial\Psi'/\partial y'$, $v'=-\partial\Psi'/\partial x'$.

The appropriate boundary conditions applied on the walls of the cavity are

$$\begin{aligned}
&x'=0,H',\quad 0\le y'\le H',\\
&\Psi'=\frac{\partial\Psi'}{\partial x'}=0,\qquad \omega'=-\frac{\partial^2\Psi'}{\partial x'^2},\qquad T'=T_c',\\
&y'=H',\quad 0\le x'\le H',\\
&\Psi'=\frac{\partial\Psi'}{\partial y'}=0,\qquad \omega'=-\frac{\partial^2\Psi'}{\partial y'^2},\qquad \frac{\partial T'}{\partial y'}=0,
\end{aligned}$$

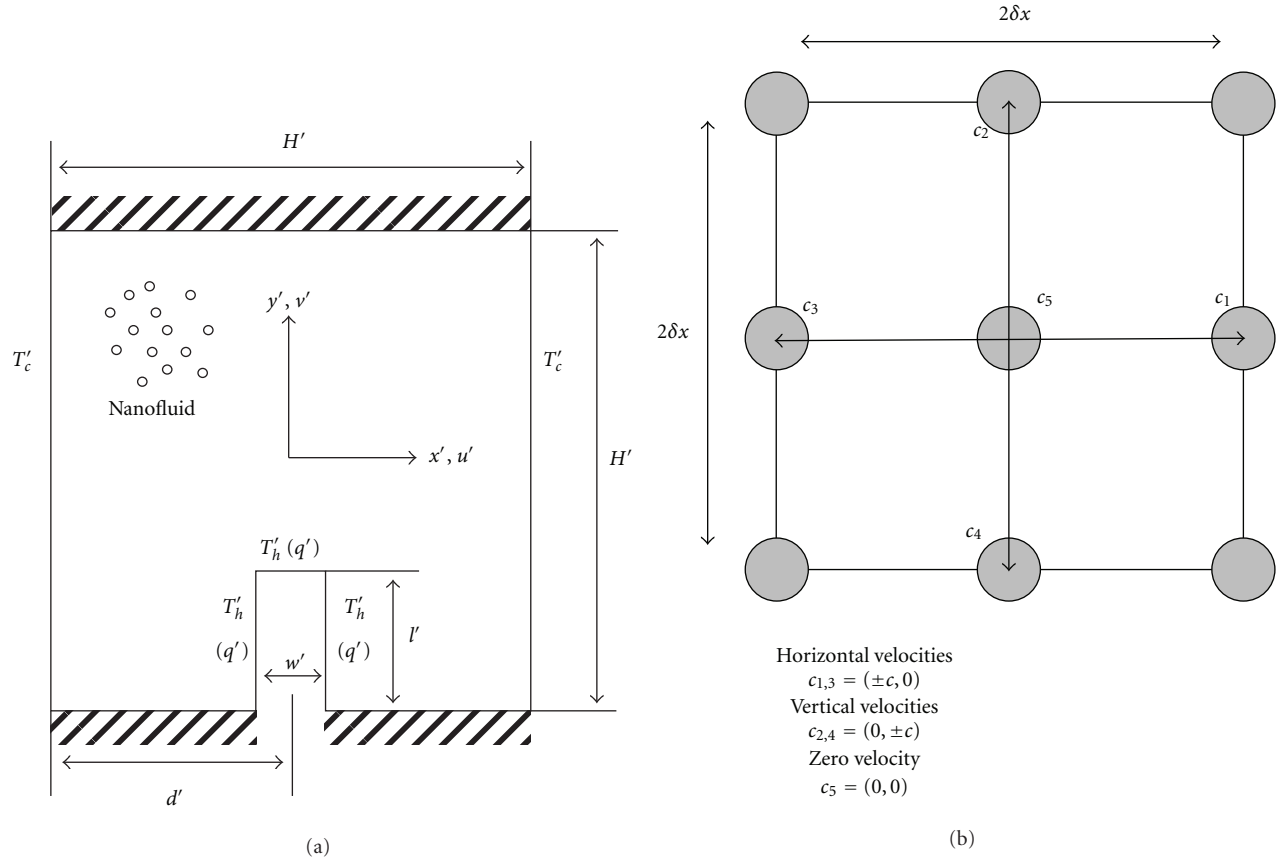

Figure 1: (a) Schematic diagram for physical model with coordinate system. (b) Diagram of the discrete D2Q5 phase space.

$$y' = 0 \quad \begin{cases} 0 \le x' \le d' - \dfrac{w'}{2} \\ d' + \dfrac{w'}{2} \le x' \le H', \end{cases}$$

$$\Psi' = \frac{\partial \Psi'}{\partial y'} = 0, \qquad \omega' = -\frac{\partial^2 \Psi'}{\partial y'^2}, \qquad \frac{\partial T'}{\partial y'} = 0. \tag{2}$$

On the heater walls, the hydrodynamic boundary conditions are given by

$$\Psi' = \frac{\partial \Psi'}{\partial n'} = 0, \qquad \omega' = -\frac{\partial^2 \Psi'}{\partial n'^2}, \tag{3}$$

while the two following thermal boundary conditions are considered:

(1) a constant temperature T'_h, such that

$$T' = T'_h, \tag{4}$$

(2) a constant heat flux q', such that

$$\frac{\partial T'}{\partial n'} = -\frac{q'}{k_{\mathrm{nf}}}. \tag{5}$$

In these equations, n' represents the normal to the heater walls, and the constant k_{nf} is the characteristic thermal conductivity of the fluid considered.

The effective density of the nanofluid is given as

$$\rho_{\mathrm{nf}} = (1 - \Phi)\rho_f + \Phi \rho_{\mathrm{np}}, \tag{6}$$

where Φ is the solid volume fraction of nanoparticles.

The thermal diffusivity of the nanofluid is

$$\alpha_{\mathrm{nf}} = \frac{k_{\mathrm{nf}}}{(\rho C_P)_{\mathrm{nf}}}, \tag{7}$$

where the heat capacitance of the nanofluid is given by

$$(\rho C_P)_{\mathrm{nf}} = (1 - \Phi)(\rho C_P)_f + \Phi (\rho C_P)_{\mathrm{np}}. \tag{8}$$

The thermal expansion coefficient of the nanofluid can be determined by:

$$(\rho \beta')_{\mathrm{nf}} = (1 - \Phi)(\rho \beta')_f + \Phi (\rho \beta')_{\mathrm{np}}. \tag{9}$$

The effective dynamic viscosity of the nanofluid is calculated using Brinkman's model [17] as follows:

$$\mu_{\mathrm{nf}} = \frac{\mu_f}{(1 - \Phi)^{2.5}}, \tag{10}$$

which gives an estimation of the viscosity of a nanofluid containing a dilute suspension of small, rigid, spherical particles.

The thermal conductivity of the nanofluid is calculated using a model proposed by Patel et al. [18] as follows:

$$\frac{k_{\mathrm{nf}}}{k_f} = 1 + \frac{k_{\mathrm{np}}A_{\mathrm{np}}}{k_f A_f} + ck_{\mathrm{np}}Pe\frac{A_{\mathrm{np}}}{k_f A_f}, \tag{11}$$

where $c = 25000$ is a constant determined experimentally, and A_{np}/A_f is defined as

$$\frac{A_{\mathrm{np}}}{A_f} = \frac{d_f}{d_{\mathrm{np}}}\frac{\Phi}{(1-\Phi)}, \tag{12}$$

with d_{np} being the diameter of the solid nanoparticles in the fluid, assumed here to be equal to $d_{\mathrm{np}} = 100\,\mathrm{nm}$, and $d_f = 2\,\mathrm{A}^\circ$ being the size of the liquid molecules, namely, those of water.

The Péclet number in (11) is defined as

$$Pe = \frac{u_{\mathrm{np}}d_{\mathrm{np}}}{\alpha_f}, \tag{13}$$

with u_{np} expressing the Brownian motion velocity of nanoparticle, defined as

$$u_{\mathrm{np}} = \frac{2k_bT'}{\pi\mu_f d_{\mathrm{np}}^2}, \tag{14}$$

where $k_b = 1.38065 \times 10^{-23}$ is the Boltzmann constant.

The governing equations with the above models are made dimensionless by scaling the length by H' and the velocity by $\alpha_f \mathrm{Ra}^{1/2}/H'$, with α_f being the thermal diffusivity of pure fluid, and time by $H'^2/\alpha_f\mathrm{Ra}^{1/2}$. Also, we introduce the reduced temperature $T = (T' - T'_0)/\Delta T'$, where $\Delta T' = (T'_h - T'_c)$ for an isothermal heater and $\Delta T' = q'H'/k_f$ for a heater with a constant heat flux. The wall temperature of the enclosure is set arbitrarily to $T'_0 = 22^\circ\mathrm{C}$, and the characteristic temperature difference is fixed to $\Delta T' = 30^\circ\mathrm{C}$.

The dimensionless equations governing the present problem then read

$$\frac{\partial^2\Psi}{\partial x^2} + \frac{\partial^2\Psi}{\partial y^2} = -\omega, \tag{15}$$

$$\frac{\partial\omega}{\partial t} + u\frac{\partial\omega}{\partial x} + v\frac{\partial\omega}{\partial y} = \overline{\nu}\frac{\mathrm{Pr}}{\mathrm{Ra}^{1/2}}\left(\frac{\partial^2\omega}{\partial x^2} + \frac{\partial^2\omega}{\partial y^2}\right) + \overline{\beta}\,\mathrm{Pr}\frac{\partial T}{\partial x}, \tag{16}$$

$$\frac{\partial T}{\partial t} + u\frac{\partial T}{\partial x} + v\frac{\partial T}{\partial y} = \frac{\overline{\alpha}}{\mathrm{Ra}^{1/2}}\left(\frac{\partial^2 T}{\partial x^2} + \frac{\partial^2 T}{\partial y^2}\right), \tag{17}$$

where

$$\overline{\nu} = \frac{\nu_{\mathrm{nf}}}{\nu_f}, \qquad \overline{\beta} = \frac{(\rho\beta')_{\mathrm{nf}}}{\left(\rho_{\mathrm{nf}}\beta'_f\right)}, \qquad \overline{\alpha} = \frac{\alpha_{\mathrm{nf}}}{\alpha_f}. \tag{18}$$

The corresponding boundary conditions are

$$x = 0, 1, \quad 0 \le y \le 1,$$
$$\Psi = \frac{\partial\Psi}{\partial x} = 0, \qquad \omega = -\frac{\partial^2\Psi}{\partial x^2}, \qquad T = 0,$$
$$y = 1, \quad 0 \le x \le 1,$$
$$\Psi = \frac{\partial\Psi}{\partial y} = 0, \qquad \omega = -\frac{\partial^2\Psi}{\partial y^2}, \qquad \frac{\partial T}{\partial y} = 0, \tag{19}$$
$$y = 0 \quad \begin{cases} 0 \le x \le D - \dfrac{W}{2} \\ D + \dfrac{W}{2} \le x \le 1, \end{cases}$$
$$\Psi = \frac{\partial\Psi}{\partial y} = 0, \qquad \omega = -\frac{\partial^2\Psi}{\partial y^2}, \qquad \frac{\partial T}{\partial y} = 0,$$

and the no slip condition on the heater wall yields

$$\Psi = \frac{\partial\Psi}{\partial n} = 0, \qquad \omega = -\frac{\partial^2\Psi}{\partial n^2}, \tag{20}$$

while the dimensionless thermal boundary conditions are as follows:

(1) the constant temperature applied on the heater

$$T = 1 \tag{21}$$

(2) the constant heat flux on the heater

$$\frac{\partial T}{\partial n} = -\frac{k_f}{k_{\mathrm{nf}}}. \tag{22}$$

The heat transfer rates along the vertical walls are expressed in terms of the local and average Nusselt's numbers Nu and $\overline{\mathrm{Nu}}$, respectively. Depending on the thermal boundary conditions applied on the heater, these parameters are computed as follows:

(3) on the left vertical wall of the heater for a constant temperature,

$$\mathrm{Nu} = -\frac{k_{\mathrm{nf}}}{k_f}\frac{\partial T}{\partial x}\bigg|_{x=0}, \tag{23}$$

$$\overline{\mathrm{Nu}} = \int_0^1 \mathrm{Nu}\,dy, \tag{24}$$

(4) on the heater for a constant heat flux,

$$Nu = \frac{1}{T}\bigg|_{\mathrm{heater}}, \tag{25}$$

$$\overline{\mathrm{Nu}} = \frac{\int_{\mathrm{Heater}}\mathrm{Nu}\,dl}{\int_{\mathrm{Heater}}dl}, \tag{26}$$

with dl representing an elementary length along the walls of the heater.

From the above equations, we can see that the present problem is governed by six dimensionless parameters, namely, the thermal Rayleigh number $\mathrm{Ra} = g\beta'_f \Delta T' H'^3/\alpha_f \nu_f$, the Prandtl number $\mathrm{Pr} = \nu_f/\alpha_f$, the solid volume fraction of nanoparticles Φ, and the geometrical parameters for the heater, that is, $L = (l'/H')$, $W = (w'/H')$, and $D = (d'/H')$. Naturally, the type of nanoparticles considered must also be specified, which introduces another parameter.

3. Numerical Solution

The solution of the governing equations, (15) to (17), is obtained using the lattice Boltzmann method (LBM). The LBM, developed two decades ago, examines fluids in the molecular state instead of at the classical macroscopic level and makes it possible to simulate flows by solving the Boltzmann transport equation for particle distribution functions on a simplified phase space, called the lattice [19, 20].

In this study, we used the LBM to solve the stream function, vorticity, and temperature equations, instead of the classical Navier-Stokes equations for velocity and temperature. This approach, recently proposed by Chai and Shi [21] and Chen et al. [22, 23], enables us to solve the advection-diffusion equations, (16) and (17), and the Poisson equation, (15), using particle distribution functions and applying the lattice Boltzmann approach on the D2Q5-phase space described in Figure 1(b).

We considered three sets of particle distribution functions. One set describes the temperature T and another the vorticity ω, both of them evolving following the collision and propagation steps described by Chen et al. [22, 23]. The third set of particle distribution functions is used for the stream function Ψ and is computed by iterating the collision and propagation steps, as described by Chai and Shi [21].

The parameters characterizing the nanofluid, that is, to say thermal diffusivity $\overline{\alpha}$, kinematic viscosity $\overline{\nu}$, and thermal expansion coefficient $\overline{\beta}$, are introduced in the model with the definition of characteristic relaxation times. These characteristic parameters, which make it possible to link the macroscopic formulation of the Navier-Stokes equations to the mesoscopic formulation of the LBM, were modified to take into account the influence of the nanoparticles on the fluid in the LBM framework for the various models studied (see e.g., Guiet et al. [24]).

With the present approach, a wide range of simulations were conducted for the simulation of natural convection in partially divided square enclosures. For these simulations, the convergence was considered to be reached when the relative error on variables $V = \Psi$, ω, and T between two successive iterations, t and $t+1$, was smaller than a chosen tolerance:

$$\mathrm{ERR}_V = \frac{\sum_x \sum_y \left| V_{x,y}^{t+1} - V_{x,y}^{t} \right|}{\sum_x \sum_y \left| V_{x,y}^{t+1} \right|} < 10^{-6}. \tag{27}$$

The calculations were performed on 101×101 regular grids using D2Q5 lattices, this refinement being a good compromise between computational time and accuracy.

To check the ability of this LBM formulation to simulate flows in partially divided cavities, various simulations were conducted for pure fluid and compared with results provided by AlAmiri et al. [16]. The accuracy of the LBM was checked for various Rayleigh's numbers, Ra, in different configurations with various heights L, widths W, and positions D of an isothermal heater. The results are summarized in Table 1. Good agreement is observed, with the maximum deviation being of the order of 1.7% for the 101×101 grid. We can note that, while increasing Ra, the stream function amplitude $\Psi_{\max} - \Psi_{\min}$ reaches a maximum at $\mathrm{Ra} = 10^5$ and then decreases. This can be explained by the fact that, increasing $\mathrm{Ra} < 10^5$, the conduction is not negligible compared to the convection; the presence of the heater affects more and more fluid in the cavity (by conduction) inducing a convection of more and more fluid in the cavity. A maximum is reached where all the fluid in the cavity is convected. Then, increasing Ra, the conduction becomes negligible, and the convection occurs more and more close from the vertical walls (cooled fluid) and above the heater (warmed fluid), leaving larger areas of the cavity where the fluid is not affected by the convection. The stream function amplitude $\Psi_{\max} - \Psi_{\min}$ tends to reduce ($\mathrm{Ra} > 10^5$).

4. Results and Discussion

The results presented in this paper were obtained for pure fluid and a copper (Cu)-water mixture. The thermophysical properties of the base fluid, that is, water, and the nanoparticles, are reported in Table 2. Since this study is limited to water-based solutions, it is assumed that the Prandtl number (Pr) equals 7. As discussed by many authors (see, e.g., Trevisan and Bejan [25]), this type of convective heat transfer is independent of this parameter, provided that this latter is of order one or greater. The results are presented for Rayleigh's numbers varying from 10^3 to 10^6, for various geometries, $0.25 \le L \le 0.8$, $0.1 \le W \le 0.8$, and positions, $0.15 \le D \le 0.5$, of the heater, while the nanoparticle volume fraction covers the $0 \le \Phi \le 0.05$ range.

Typical numerical results are presented in Figure 2 for $\mathrm{Ra} = 10^5$, $D = 0.5$, and $W = 0.2$. On the graphs, streamlines and isotherms are presented from left to right. The calculated maximum stream functions ($|\Psi_{\max}|$) and heat transfer ($\overline{\mathrm{Nu}}$) are also given with each graph for reference. In these figures, the streamlines are equally spaced between $\Psi = 0$ on the boundaries and the maximum (minimum) value $\Psi_{\max}$ ($\Psi_{\min}$). Also, the isotherms are equally spaced between $T_{\max} = 1$ and $T_{\min} = 0$. Figure 2(a) shows the results obtained for a cavity with a protruding isothermal heater of height $L = 0.25$, filled with a pure solution ($\Phi = 0$). The resulting flow and temperature fields are similar to those reported in the literature in the past (see, e.g., AlAmiri et al. [16]). Since the heater is centrally located in the middle of the bottom wall ($D = 0.5$), symmetrical flow and temperature patterns, about a vertical line passing

Table 1: Comparison with results provided by Alimiri et al. [16] of the stream function extremes (Ψ_{min}, Ψ_{max}) for various heat source configurations (Pr = 0.71).

Ra	W	L	D	Reference [16]	Present	Difference
10^4	0.2	0.25	0.5	$(-0.0333, 0.0333)$	$(-0.0330, 0.0330)$	0.9%
10^5	0.2	0.25	0.5	$(-0.0459, 0.0459)$	$(-0.0458, 0.0458)$	0.22%
10^6	0.2	0.25	0.5	$(-0.0290, 0.0290)$	$(-0.0289, 0.0289)$	0.34%
10^6	0.1	0.25	0.5	$(-0.0292, 0.0292)$	$(-0.0291, 0.0291)$	0.34%
10^6	0.4	0.25	0.5	$(-0.0299, 0.0299)$	$(-0.0299, 0.0299)$	0%
10^6	0.2	0.05	0.5	$(-0.0331, 0.0331)$	$(-0.0330, 0.0330)$	0.34%
10^6	0.2	0.5	0.5	$(-0.0239, 0.0239)$	$(-0.0235, 0.0235)$	1.7%
10^6	0.2	0.25	0.2	$(-0.0334, 0.0288)$	$(-0.0328, 0.0286)$	1.3%

Table 2: Thermophysical properties of water and Cu-nanoparticles [8].

	ρ (kg m^{-3})	C_p (J kg^{-1} K^{-1})	k (Wm^{-1} K^{-1})	$\beta\times10^5$ (K^{-1})
H_2O	997.1	4179	0.613	21
Cu	8933	385	401	1.67

through the axis of symmetry of the heated element, are observed in the enclosure. The streamlines are seen to occupy the entire cavity body. The field of isotherms indicates that these are mostly parallel to the heated and cooled boundaries, except above the heated element. As the solid volume fraction is increased to $\Phi = 0.05$, the resulting streamlines and isotherms are depicted as in Figure 2(b). It is found that, as expected, the flow and temperature patterns are influenced by the addition of nanoparticles, which enhances the buoyancy forces, owing to the increase in the effective thermal conductivity of the mixture. As a result, the strength of convective heat transfer is improved with an increase in solid concentration. In fact, the increase in the Nusselt number is about 33.5% for a concentration of nanoparticles as low as $\Phi = 0.05$. Figure 2(c) shows the results obtained when the heater height is increased to $L = 0.50$ for $\Phi = 0.05$. A comparison between Figures 2(b) and 2(c) indicates that, as the height of the heater increases, the intensity of the convective motion diminishes, as indicated by the values of the maximum and minimum stream function patterns. This is because an increase in the length of the heated element results in an increase in resistance to the flow. However, the average Nusselt-number is found to be enhanced from $\overline{\mathrm{Nu}} = 4.356$ to $\overline{\mathrm{Nu}} = 5.839$ as the heater height is increased from $L = 0.25$ to $L = 0.50$. Similar data were obtained for the same conditions, but for the case of a block heated by a constant heat flux. The obtained results (not presented here) indicate that the streamline patterns were qualitatively similar to those reported for the isothermal heater. Naturally, the isotherm patterns are quite different, especially in the vicinity of the heater, where the surface temperature of this latter is not constant.

Figure 3 illustrates the variation in $\overline{\mathrm{Nu}}$ with the solid volume fraction Φ at various Rayleigh's numbers. The specific geometrical configuration of the heating source considered is $D = 0.5$, $L = 0.25$, and $W = 0.2$. The results obtained for the isothermal heater and the constant heat flux heater are depicted in Figures 3(a) and 3(b), respectively. In general, past studies on this topic have demonstrated that the addition of nanoparticles to a base fluid leads to the occurrence of two opposing effects on the convective heat transfer within the cavity. The first effect, resulting from the enhanced thermal conductivity of the mixture owing to the presence of the nanoparticles, improves $\overline{\mathrm{Nu}}$. The second effect,owing to the increase in viscosity caused by the addition of nanoparticles, eliminates the convective motion and thusreduces $\overline{\mathrm{Nu}}$. Which of these two antagonist mechanisms prevails depends on the type of particles used, the convection intensity (Ra), and the models considered to approximate the viscosity and thermal conductivity of the mixture. In this study, the results depicted in Figure 3 show that, for a given Ra value, a monotonic increase in $\overline{\mathrm{Nu}}$ is obtained with the addition of nanoparticles. For the isothermal heater, Figure 3(a) indicates that, at $\Phi = 0.05$, the Nusselt number is enhanced by about 38% for $\mathrm{Ra} = 10^3$ and by about 32% for $\mathrm{Ra} = 10^6$. The case of a constant heat flux heater, Figure 3(b), is discussed next. For this situation, the temperatures of the surface of the heater, T, are not constant. As a matter of fact, its maximum value, T_{max}, is an important parameter in the thermal design of electronic devices. For a given value of Φ, Figure 3(b) shows that increasing monotonically Ra enhances $\overline{\mathrm{Nu}}$. This follows from the fact that increasing the Rayleigh number enhances convection, that is, heat removal from the heater. As a result, the temperatures on the surface of the heated element are reduced, resulting in an enhancement of the heat transfer. Specifically, it is found that, at $\Phi = 0.05$, the Nusselt number is enhanced by about 36% for $\mathrm{Ra} = 10^3$ and by about 22% for $\mathrm{Ra} = 10^6$. Note that in that case the computed average Nusselt numbers for $\mathrm{Ra} = 10^3$ and 10^4 are almost identical. This is due to the weak impact of natural convection on the heat transfer for these two cases, the heat exchange being due to conduction. The impact of the convection starts appearing for the simulations at $\mathrm{Ra} = 10^5$.

This result indicates that the cooling performance of nanofluids is more effective at low Rayleigh's numbers than at

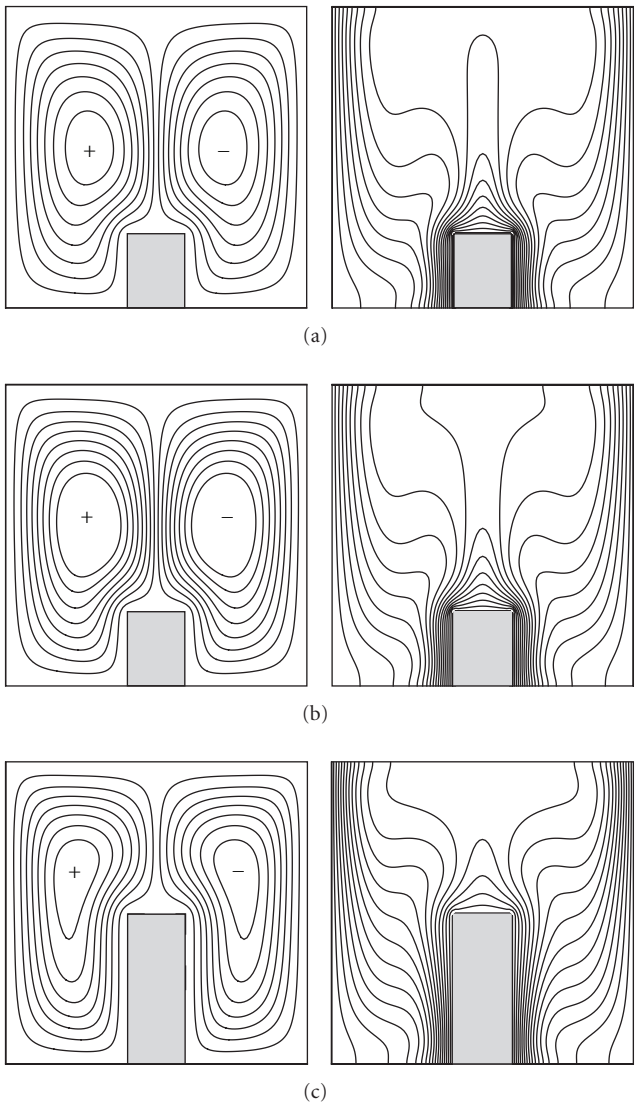

Figure 2: Effect of varying the ratio of nanoparticles, Φ, and the length, L, of an isothermally heated heater on the streamlines (left) and isotherms (right) for $\mathrm{Ra} = 10^5$, $D = 0.5$, $W = 0.2$, and (a) $L = 0.25$ and $\Phi = 0$: $|\Psi_{\max}| = 0.0391$, $\overline{\mathrm{Nu}} = 3.264$, (b) $L = 0.25$ and $\Phi = 0.05$: $|\Psi_{\max}| = 0.0506$, $\overline{\mathrm{Nu}} = 4.356$, (c) $L = 0.50$ and $\Phi = 0.05$: $|\Psi_{\max}| = 0.0392$, $\overline{\mathrm{Nu}} = 5.839$.

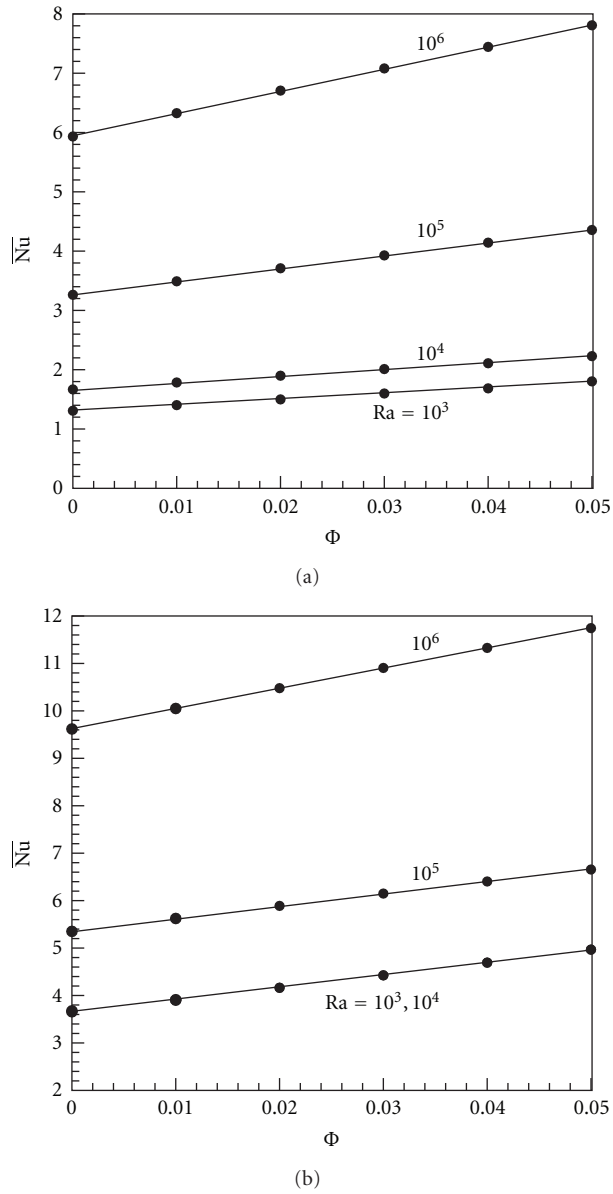

Figure 3: Variation of the average Nusselt number $\overline{\mathrm{Nu}}$ with solid volume fraction Φ at various Rayleigh's number's Ra for $D = 0.5$, $L = 0.25$, $W = 0.2$, and for, (a) isothermal heater; (b) heater with a constant heat flux.

high ones, independently of the heating conditions imposed on the heater. This behavior of $\overline{\mathrm{Nu}}$ with Φ is in good agreement with the results reported in previous studies, especially when the Rayleigh number is small enough that convection is weak ($\mathrm{Ra} \leq 10^4$). For this situation, for which heat transfer by conduction prevails, the increase in $\overline{\mathrm{Nu}}$ with Φ is due to the enhancement in thermal conductivity of the nanofluid. This trend has been found to be independent of the models used to characterize the mixture. It must be mentioned that a review of the literature indicates that, at higher Ra values for which heat transfer is dominated by convection, the effects of the nanoparticle volume fraction on the Nusselt number was found to be either beneficial or detrimental, depending on the formulas adopted to model the effective thermal conductivity and dynamic viscosity of the nanofluid.

Figure 4 illustrates the variation of $\overline{\mathrm{Nu}}$ for $\mathrm{Ra} = 10^5$, in terms of the geometry and position of the heat source and Φ of the mixture, for a heater with a constant heat flux. Figures 4(a) and 4(b) show the variation of $\overline{\mathrm{Nu}}$ with the height L of the heated element. It can be seen that, for a given solid volume fraction, the Nusselt number decreases as the height increases. This follows from the fact that the temperature at the surface of the element increases as the height of the element increases, owing to the higher heat flux generated by the heat source. The influence of the heater width W on $\overline{\mathrm{Nu}}$ is presented in Figure 4(b). For a given Φ, it is found

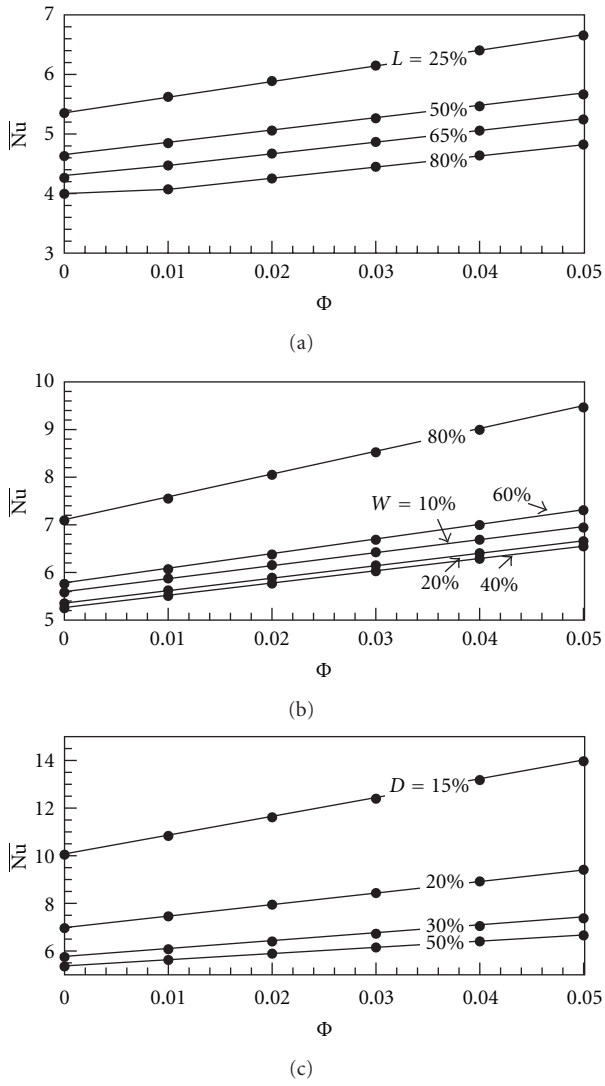

Figure 4: Variation of the average Nusselt number $\overline{\text{Nu}}$, for the case of a heater with a constant heat flux, with solid volume fraction Φ for $\text{Ra} = 10^5$: (a) effect of the heater height L for $D = 0.5$ and $W = 0.2$; (b) effect of the heater width W for $D = 0.5$ and $L = 0.25$; (c) effect of the heater position D for $L = 0.25$ and $W = 0.2$.

that, as the width of the heater increases from $W = 0.10$ to $W = 0.80$, the Nusselt number first decreases to reach a minimum at about $W = 0.40$. Above this value, $\overline{\text{Nu}}$ is found to increase sharply with W. Concerning the influence of Φ, Figure 4(a) indicates that, with an increase of 5% in this parameter, the Nusselt number grows by about 24% at $L = 0.25$ and by about 21% at $L = 0.80$. Similarly, it is observed from Figure 4(b) that $\overline{\text{Nu}}$ improves by 24% at $W = 0.10$ and 33% at $W = 0.80$. Figure 4(c) presents the effect of the location of the heat source D on $\overline{\text{Nu}}$. Independently of the concentration Φ of the solution, the average Nusselt number is minimum for $D = 0.50$, that is, when the heater is centrally located at the bottom of the enclosure. Naturally, symmetrical flow and temperature patterns are generated in the enclosure in this case (Figure 5(a)). As the heat source moves towards the left vertical isothermal wall ($D < 0.5$), the flow patterns consist of two nonsymmetrical counterrotating cells of unequal strengths (Figures 5(b) and 5(c)). The isotherm patterns indicate that, as the heater is moved to the left cold wall, the temperature of the heat source, which is not uniform since it is heated by a constant heat flux, decreases. Moving the heat source to the vicinity of the cooled boundary enhances heat removal considerably, which reduces the temperatures on the surface of the heater. As a result, the average Nusselt number increases sharply as it moves away from the central position, $D = 0.50$. Also, Figure 4(c) shows that the average Nusselt number increases monotonically with the solid volume, independently of the position of the heater. With an increase of 5% in solid volume fraction, the Nusselt number grows by about 40% at $D = 0.15$ and by about 24% at $D = 0.5$.

Figure 6 illustrates the results obtained for the same conditions as those of Figure 4, but for the case of an isothermal heater. A bird's eye view of the graphs indicates that, independently of the geometry and position of the heat source, the Nusselt number increases with an increase in the volume fraction Φ, that is, the thermal conductivity of the solution. Thus, as expected, this behavior is independent of the thermal boundary conditions applied on the heat source. The effect of the size of the heater on heat transfer is shown in Figures 6(a) and 6(b), which indicate that $\overline{\text{Nu}}$ improves with an increase in the dimensions of the heating surface. The fact that the average Nusselt number improves with an increase in the height and width of an isothermal heater located at the bottom of a cavity has already been reported by AlAmiri et al. [16] for pure fluid. The influence of the position D of the block heater on the heat transfer is depicted in Figure 6(c). Qualitatively, the results are similar to those reported for the case of the block when heated by a constant heat flux (Figure 4(c)). Quantitatively, Figure 6(c) indicates that, when Φ increases from 0 to 5%, the Nusselt number grows by about 35% at $D = 0.15$ and by about 33% at $D = 0.5$.

5. Conclusions

In this paper, a numerical study of natural convection heat transfer in a square enclosure filled with a suspension of copper-water nanofluid is carried out. The simulations were performed using the lattice Boltzmann approach. The system is heated, by a protruding heater located at the bottom of the system, and cooled isothermally from the two vertical walls. The heater is assumed either to be isothermal or to generate a constant heat flux. The governing parameters of the problem are the thermal Rayleigh number, Ra, the solid volume fraction of nanoparticles, Φ, the size (L and W) of the heater and its position, D. The main conclusions of the present analysis are as follows.

(1) In the range of the governing parameters considered in this study, for a given geometry and position of the heater, the heat transfer is improved by enhancing both the Rayleigh number and the nanoparticle volume fraction.

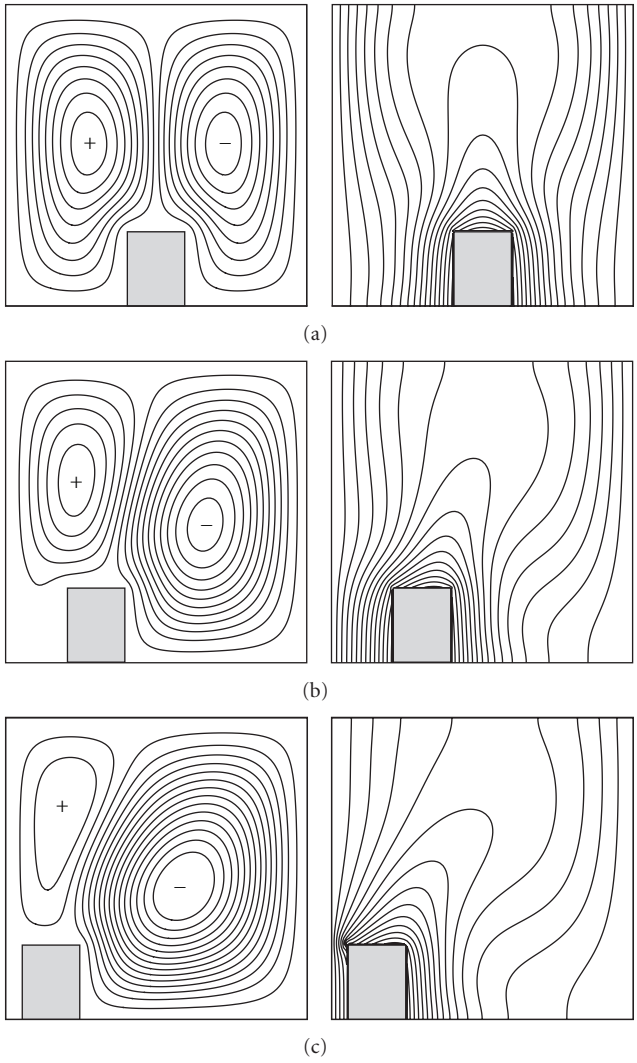

Figure 5: Effect of varying the position D of the constant heat flux heater on the streamlines (left) and isotherms (right) for Ra = 10^5, $\Phi = 0.05$, $L = 0.25$, $W = 0.2$ and: (a) $D = 0.50$: $\Psi_{max} = 0.0153$, $\Psi_{min} = -0.0153$, $T_{max} = 0.1677$, $\overline{Nu} = 6.6556$; (b) $D = 0.30$: $\Psi_{max} = 0.0092$, $\Psi_{min} = -0.0190$, $T_{max} = 0.1526$, $\overline{Nu} = 7.3719$; (c) $D = 0.15$: $\Psi_{max} = 0.0036$, $\Psi_{min} = -0.0199$, $T_{max} = 0.1476$, $\overline{Nu} = 13.9672$.

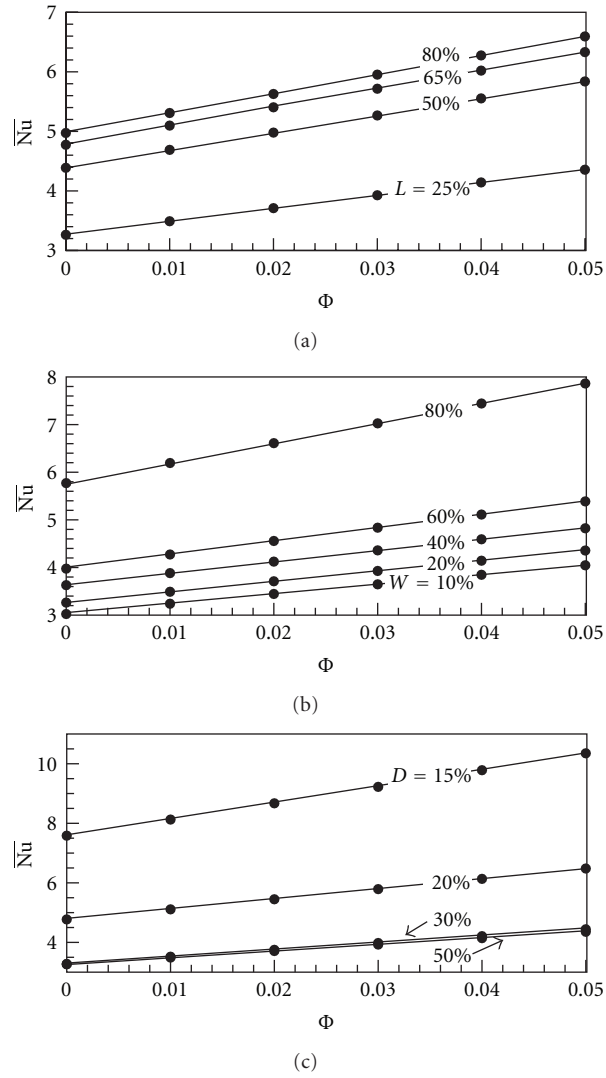

Figure 6: Variation of the average Nusselt number $\overline{Nu}$ (computed on the left vertical wall), for an isothermal heater, with solid volume fraction Φ for Ra = 10^5: (a) effect of the heater height L for $D = 0.5$ and $W = 0.2$; (b) effect of the heater width W for $D = 0.5$ and $L = 0.25$; (c) effect of the heater position D for $L = 0.25$ and $W = 0.2$.

(2) For the case of an isothermal heater, the numerical results indicate that, for a given solid volume fraction of nanoparticles, the heat transfer is improved when the size of the heating source increases. Also, the average Nusselt number is enhanced as the position of the heating block is moved from the center position toward the vertical isothermal boundaries of the enclosure.

(3) For the case of a heater with a constant heat source, for a given Rayleigh number and solid volume fraction of nanoparticles, the increase in the height of the heater results in a rise in the maximum surface temperature of the element. Consequently, the average Nusselt number decreases with the increase in the height of the heat source. The influence of the width, W, on $\overline{Nu}$ is more complex. When it increases from $W = 0.1$, $\overline{Nu}$ first decreases to reach a minimum at $W \approx 0.4$, above which the heat transfer increases monotonically with W. As in the case of the isothermal heater, as the position D of the heating block is moved from the center of the bottom wall of the cavity towards the left (right) vertical cooled wall, the maximum temperature of the element decreases, which improves $\overline{Nu}$.

Nomenclature

C_p: Heat capacitance
D: Dimensionless location of the heater (d'/H')

d': Distance of the heat element from the left wall
d_{np}: Diameter of a solid nanoparticle
d_f: Diameter of a liquid molecule
g: Gravitational acceleration
H': Height of cavity
k: Thermal conductivity
k_b: Boltzmann's constant ($k_b = 1.38065 \times 10^{-23}$)
L: Dimensionless height of the heater (l'/H')
l': Height of the heater
Nu: Nusselt number (23) and(25)
$\overline{\text{Nu}}$: Average Nusselt number (24) and(26)
Pe: Péclet number, ($u_{np}d_{np}/\alpha_f$)
Pr: Prandtl number of pure fluid (ν_f/α_f)
q' Constant heat flux per unit area
Ra: Thermal Rayleigh number ($g\beta'_f\Delta T'H'^3/\alpha_f\nu_f$)
t: Dimensionless time ($t'\alpha_f \text{Ra}^{1/2}/H'^2$)
T: Dimensionless temperature ($(T' - T'_0)/\Delta T'$)
T'_0: Reference temperature
u: Dimensionless velocity in x direction ($u'H'/\alpha_f \text{Ra}^{1/2}$)
u_{np}: Brownian motion velocity of nanoparticles
v: Dimensionless velocity in y direction ($v'H'/\alpha_f \text{Ra}^{1/2}$)
W: Dimensionless width of the heater (w'/H')
w': Width of the heater
x: Dimensionless coordinate axis (x'/H')
y: Dimensionless coordinate axis (y'/H').

Greek Symbols

α: Thermal diffusivity
$\overline{\alpha}$: Dimensionless parameter (α_{nf}/α_f)
β': Thermal expansion coefficient
$\overline{\beta}$: Dimensionless parameter ($(\rho\beta')_{nf}/(\rho\beta')_f$)
ν: Kinematic viscosity of fluid
$\overline{\nu}$: Dimensionless parameter (ν_{nf}/ν_f)
ρ: Density of fluid
Φ: Nanoparticle volume fraction
Ψ: Dimensionless stream function ($\Psi'/\alpha_f \text{Ra}^{1/2}$)
ω: Dimensionless vorticity ($\omega'/\alpha_f \text{Ra}^{1/2}$).

Subscript

0: Reference state
f: Pure fluid
max: Maximum values
min: Minimum values
nf: Nanofluid
np: Nanoparticle.

Superscript

$'$: It refers to a dimensional variable.

References

[1] S. U. S. Choi, "Enhancing thermal conductivity of fluids with nanoparticles," *Flow*, vol. 66, pp. 99–105, 1995.

[2] L. Godson, B. Raja, D. Mohan Lal, and S. Wongwises, "Enhancement of heat transfer using nanofluids—an overview," *Renewable and Sustainable Energy Reviews*, vol. 14, no. 2, pp. 629–641, 2010.

[3] K. Khanafer, K. Vafai, and M. Lightstone, "Buoyancy-driven heat transfer enhancement in a two-dimensional enclosure utilizing nanofluids," *International Journal of Heat and Mass Transfer*, vol. 46, no. 19, pp. 3639–3653, 2003.

[4] R. Y. Jou and S. C. Tzeng, "Numerical research of nature convective heat transfer enhancement filled with nanofluids in rectangular enclosures," *International Communications in Heat and Mass Transfer*, vol. 33, no. 6, pp. 727–736, 2006.

[5] C. J. Ho, M. W. Chen, and Z. W. Li, "Numerical simulation of natural convection of nanofluid in a square enclosure: effects due to uncertainties of viscosity and thermal conductivity," *International Journal of Heat and Mass Transfer*, vol. 51, no. 17-18, pp. 4506–4516, 2008.

[6] A. K. Santra, S. Sen, and N. Chakraborty, "Study of heat transfer augmentation in a differentially heated square cavity using copper-water nanofluid," *International Journal of Thermal Sciences*, vol. 47, no. 9, pp. 1113–1122, 2008.

[7] E. Abu-Nada, Z. Masoud, H. F. Oztop, and A. Campo, "Effect of nanofluid variable properties on natural convection in enclosures," *International Journal of Thermal Sciences*, vol. 49, no. 3, pp. 479–491, 2010.

[8] E. Abu-Nada, Z. Masoud, and A. Hijazi, "Natural convection heat transfer enhancement in horizontal concentric annuli using nanofluids," *International Communications in Heat and Mass Transfer*, vol. 35, no. 5, pp. 657–665, 2008.

[9] B. Ghasemi and S. M. Aminossadati, "Periodic natural convection in a nanofluid-filled enclosure with oscillating heat flux," *International Journal of Thermal Sciences*, vol. 49, no. 1, pp. 1–9, 2010.

[10] Z. Alloui, P. Vasseur, and M. Reggio, "Natural convection of nanofluids in a shallow cavity heated from below," *International Journal of Thermal Sciences*, vol. 50, no. 3, pp. 385–393, 2011.

[11] F. Moukalled and S. Acharya, "Buoyancy-induced heat transfer in partially divided trapezoidal cavities," *Numerical Heat Transfer; Part A*, vol. 32, no. 8, pp. 787–810, 1997.

[12] F. Moukalled and M. Darwish, "Natural convection in a partitioned trapezoidal cavity heated from the side," *Numerical Heat Transfer; Part A*, vol. 43, no. 5, pp. 543–563, 2003.

[13] M. A. Coman, G. O. Hughes, R. C. Kerr, and R. W. Griffiths, "The effect of a barrier on laminar convection in a box with differentially heated endwalls," *International Journal of Heat and Mass Transfer*, vol. 49, no. 17-18, pp. 2903–2911, 2006.

[14] H. Oztop and E. Bilgen, "Natural convection in differentially heated and partially divided square cavities with internal heat generation," *International Journal of Heat and Fluid Flow*, vol. 27, no. 3, pp. 466–475, 2006.

[15] Y. Varol, H. F. Oztop, and T. Yilmaz, "Natural convection in triangular enclosures with protruding isothermal heater," *International Journal of Heat and Mass Transfer*, vol. 50, no. 13-14, pp. 2451–2462, 2007.

[16] A. AlAmiri, K. Khanafer, and I. Pop, "Buoyancy-induced flow and heat transfer in a partially divided square enclosure," *International Journal of Heat and Mass Transfer*, vol. 52, no. 15-16, pp. 3818–3828, 2009.

[17] H. C. Brinkman, "The viscosity of concentrated suspensions and solutions," *The Journal of Chemical Physics*, vol. 20, no. 4, pp. 571–581, 1952.

[18] H. E. Patel, T. Sundararajan, T. Pradeep, A. Dasgupta, N. Dasgupta, and S. K. Das, "A micro-convection model for thermal conductivity of nanofluids," *Pramana—Journal of Physics*, vol. 65, no. 5, pp. 863–869, 2005.

[19] S. Succi, *The Lattice Boltzmann Equation for Fluid Dynamics and Beyond*, Oxford University Press, Oxford, UK, 2001.

[20] D. A. Wolf-Gladrow, *Lattice-Gas Cellular Automata and Lattice Boltzmann Models: An Introduction*, Springer, Berlin, Germany, 2000.

[21] Z. Chai and B. Shi, "A novel lattice Boltzmann model for the Poisson equation," *Applied Mathematical Modelling*, vol. 32, no. 10, pp. 2050–2058, 2008.

[22] S. Chen, J. Tölke, and M. Krafczyk, "Simulation of buoyancy-driven flows in a vertical cylinder using a simple lattice Boltzmann model," *Physical Review E*, vol. 79, no. 1, Article ID 016704, 2009.

[23] S. Chen, J. Tölke, and M. Krafczyk, "Simple lattice Boltzmann subgrid-scale model for convectional flows with high Rayleigh numbers within an enclosed circular annular cavity," *Physical Review E*, vol. 80, no. 2, Article ID 026702, 2009.

[24] J. Guiet, M. Reggio, P. Vasseur, and S. Leclaire, "Application of the lattice Boltzmann method to calculate the natural convection of nanofluids in a shallow cavity," in *Proceedings of the 18th Annual Conference of the CFD Society of Canada*, 2010.

[25] O. V. Trevisan and A. Bejan, "Natural convection with combined heat and mass transfer buoyancy effects in a porous medium," *International Journal of Heat and Mass Transfer*, vol. 28, no. 8, pp. 1597–1611, 1985.